



Spatial arrangement of the animal male germ cell genome: III. A new experimental evidences in support of the Megarosette-loop model of spatial organization of chromo- somes in *Drosophila* sperm genome

Igor D. Alexandrov^{1,2*}, Margarita V. Alexandrova^{1,2}, Victor A. Stepanenko³, Svetlana V. Korablinova¹, Larisa N. Korovina¹ and Stanislav G. Stetsenko⁴

¹ Dzhelepov Laboratory of Nuclear Problems, Joint Institute for Nuclear Research, 141980 Dubna, Moscow Region, Russia

² Vavilov Institute of General Genetics, Russian Academy of Sciences, 119991, Moscow, Russia

³ Laboratory of Information Technologies, Joint Institute for Nuclear Research

⁴ Laboratory of High Energy, Joint Institute for Nuclear Research

Abstract

The data on the non-random pattern of induction of the *black (b)* inversions in autosome 2 after action of γ -rays of ⁶⁰Co or 0.85 MeV fission neutrons on *Drosophila* mature spermatozoa were described and 2D model of spatial arrangement of this autosome in sperm nucleus at the time of irradiation based on these data was presented. The main features of this model found to be entirely consistent with the chromosome macroarchitecture proposed earlier on the basis of data for the *vestigial (vg)* inversions at the same autosome.

*Correspondence Author:

Dzhelepov Laboratory of Nuclear Problems, Joint Institute for Nuclear Research, Dubna 141980, Moscow Region, Russia
E-mail: igdon@jinr.ru

Received: March 5, 2008; Accepted: March 17, 2008.

A general 2D and 3D models for the specific megarosette-loop structure of autosome in question with both sets of the inversion data were constructed validity of which was independently confirmed by the induction patterns of inversions not associated with the locus-specific mutations under study.

It is stated that there are all reasons to believe that all other chromosomes in sperm genome have the same spatial macroarchitecture as the most compact and suitable one to pass on the genetic information from one generation to another. It is particularly emphasized that large-scale chromosome geometry proposed is fundamentally unlike Rabl's configuration of interphase chromosomes in animal somatic cells. The conversion of Rabl's configuration to megarosette-loop structure is presumed to keep pace with protein remodeling of chromatin in late spermiogenesis.

Key words: Radiation, inversions, 2D/3D models of haploid chromosome, sperm genome, *Drosophila*.

Introduction

As it has already been intimated (Alexandrov *et al.*, 2007a,b), many modern models that provide an explanation for the large-scale geometry of chromosomes in interphase nuclei of animal and plant somatic cells reproduce or elaborate in more detail, based on the recent advances in molecular biology combined with high-resolution *in situ* hybridization, an idea originally proposed by Rabl (1885) more than 120 years ago, namely, that the chromosomes occupy distinct nuclear domains throughout the cell cycle and have polar configuration with centromeric and telomeric regions located at the opposite sides of the nucleus.

The spatial organization of chromosomes in animal sperm genome remains a mystery so far and we pioneered in the study of this issue using the analysis of radiation-induced inversions as indicators of large-scale DNA geometry in *Drosophila* sperm nuclei considering the fact that the formation of inversions requires the spatial proximity of its ends. Hereat, a special feature of our approach is that only locus-specific inversions in which one of the inversion breaks invariably associated with one or other marker genetic loci have been selected and analysed. The results obtained for a large set of inversions associated with the *vg* gene located in the middle of 2R arm of *Drosophila* autosome 2 have clearly indicated non-random proximity of this genetic region with the three distinct areas of autosome (centromeric heterochromatin and both telomeric ends) showing hereby that the large-scale geometry of haploid autosome 2 in *Drosophila* sperm genome is not described by the polar Rabl's configuration but rather it follows to the specific megarosette-loop structure the general principles of 2D-3D organization of which were modeled and represented previously (Alexandrov *et al.*, 2007b).

However, the experimental data based on the *vg* inversions only give no way of deducing the spatial configuration of the entire 2L arm as well as of the rest chromosome areas modeled as "giant" loops.

Here, a new experimental findings giving an insight into these issues and supporting the model proposed as a whole are presented by focusing into the samples of inversions associated with the *black* (*b*) gene in the middle of 2L arm (section 34D5 on the polytene chromosome) as well as of ones arising independently and simultaneously with the "point" locus-specific mutations under study at the same autosome 2.

Materials and Methods

Random set of γ -ray and neutron-induced *b* inversions (Table 1) in which one of the inversion breakpoints has invariably associated with the *b* gene was obtained at the same experiments in parallel with the *vg* inversions described earlier (Alexandrov *et al.*, 2007a). The main results of the fine genetical and cytogenetical analysis of these *b* inversions have been presented too elsewhere (Alexandrov and Alexandrova, 1991). Here it is worth noting that the precise chromosome location of the second inversion breakpoints was performed by the standard cytological technique for *Drosophila* polytene chromosomes in the mutant chromosome/wild-

type chromosome heterozygotes and estimated accurately within subsection of the polytene autosome 2 guided by its classical map under the light microscopy (Lefevre, 1976).

In parallel with the *b* and *vg* inversions, random samples of radiation-induced inversions with breakpoints outside of the *b*, *cn* and *vg* loci were obtained during the same experiments as the intrachromosomal exchanges attendant with the "point" mutations at the genetic loci under study (Table 2). The fine, within subsection, mapping of breakpoints underlying these exchanges was carried out using the same standard cytological technique too. The close examination of the breakpoint distribution for these inversions is of great interest to assess the validity of the model proposed.

Results and Discussion

The *black* inversions

According to a great body of experimental data on the comparative radiomutability of different genetic loci in *Drosophila* collected during our large-scale experiments, the *b* region (a middle of 2L arm of autosome 2), unlike the *vg* one (a middle of 2R arm of the same autosome), is not taken an active part in para- or pericentric inversions in sperm nuclei irradiated. For example, altogether 60 out of 198 (30.3%) γ -ray – or neutron-induced *vg* mutants scored and precisely analysed (Alexandrov *et al.*, 1997) were associated with intrachromosomal exchanges in question whereas only 17 out of 189 (9%) radiation-induced *b* mutants studied (loc. cit) were referred to such exchanges.

Nevertheless, the analysis of these *b* inversions (Table 1) enables one to note reasonably non-random pattern of distribution of the second inversion breakpoints over the autosome 2 with well-marked clustering of γ -ray- as well as neutron-induced breaks at the centromeric heterochromatin of the autosome (9 cases out of 18 or 50% taking into account the fact that the *b87e152* autosome 2 contains both para- and pericentric inversions with one break in common (at the *b* region) and, thus, a total number of the *b* inversions analysed ranges up to 18).

These findings show that a middle of 2L arm of autosome 2 marked by the *b* gene systematically interacts with centromeric heterochromatin resulting in the "giant" inversion loop comprising of the six sections

Table 1. The location of the second inversion breakpoints on the polytene autosome 2 of *D. melanogaster* for γ -ray- and neutron-induced *b* inversions (about the “first” breakpoints see text).

No	Code of <i>b</i> inversion	Radiation, dose	Location of the second inversion point
1	b71k1	γ -rays, 40 Gy	In(2LR) 43C2
2	b79d5	n, 10 Gy	In(2L) 35B10
3	b79h1	γ -rays, 40 Gy	In(2L) 40E
4	b81a	γ -rays, 40 Gy	In(2LR) 41D
5	b81f3	n, 10 Gy	In(2L) 35B10
6	b8117	γ -rays, 20 Gy	In(2L) 40F
7	b82c44	n, 10 Gy	In(2L) 40F
8	b83b22	γ -rays, 40 Gy	In(2L) 35B8
9	b87e152	γ -rays, 20 Gy	Ins(2LR) 22A, 34D, 41A
10	b88e1	n, 10 Gy	In(2LR) 43E
11	b88e16	n, 10 Gy	In(2L) 36C10
12	b88e32	n, 10 Gy	In(2L) 40C
13	b88e45	n, 15 Gy	In(2L) 40E
14	b88g4	n, 10 Gy	In(2LR) 56F
15	b89e64a	γ -rays, 40 Gy	In(2LR) 45F6
16	b89e100	γ -rays, 40 Gy	In(2L) 40E
17	b9119	γ -rays, 40 Gy	In(2L) 40F

Table 2. The location of the breakpoints on the polytene chromosome 2 of *D. melanogaster* for γ -ray- and neutron-induced inversions attendant with the “point” mutations at the *b*, *cn* and *vg* loci mapped at the 34D, 43E and 49E chromosomal sections, respectively.

The “point” locus-specific mutations		
<i>b</i>	<i>cn</i>	<i>vg</i>
In(2L) 33A;35E; n, 10 Gy	In(2L) 22B;36F; n, 7 Gy	In(2L) 22A;34A; γ , 40 Gy
In(2L) 35C;40A; γ , 40 Gy	In(2L) 22C;36C; γ , 40 Gy	In(2R) 41A;52D; n,10 Gy
In(2R) 41A;52A; γ , 15 Gy	In(2L) 22D;36C; γ , 60 Gy	In(2LR)35B;41D; n,15 Gy
In(2R) 41A;60A; γ , 40 Gy	In(2L) 23B;35D; n, 10 Gy	In(2L) 35D;40D; γ , 40 Gy
In(2R) 52D;60B; n, 7 Gy	In(2R) 41A;42E; γ , 40 Gy	In(2LR)39A;48E; γ , 40 Gy
	In(2R) 41D;58F; γ , 40 Gy	In(2R) 41A;50C; γ , 40 Gy
	In(2R) 50B;56B; n, 7 Gy	In(2R) 50C;56C; γ , 20 Gy

of chromosome 2L map or almost seven million pair of DNA bases (7 Mb) if it is taken into account that each section contains on average about 1.2 Mb (Adams *et al.*, 2000). Therefore, it is believed that both chromosome regions under consideration are spatially close to each other in most sperm nuclei at the time of irradiation. Remarkably, this picture faithfully copies the that described for the *vg* locus (a middle of 2R arm of the same autosome) which most frequently interacts too with centromeric heterochromatin to give rise the radiation-induced “giant” inversions (Alexandrov *et al.*, 2007a, b).

In other sperm nuclei, smaller inversions (1 – 2 Mb) with the second breakpoints in sections 35-36 are induced regularly (4/18 or 22.2 %) showing the possibility of proximity of the *b* locus with this adjacent chromosomal area.

In sum, almost 2/3 of the *b* inversions scored and analysed were based on an alternative pair-wise interaction of the *b* gene with only two chromosomal areas pointed out testifying that all of three chromosome regions being considered come within short distances of each other (within so-called “sensitive microvolume” of sperm nucleus in the vicinity of 2L arm centromeric heterochromatin). In such an event, the occurrence of a particular inversion should probably reflect the most degree of the spatial proximity as well as the realized probability of induced contact and interaction for two given regions in the given sperm nucleus irradiated.

The rest *b* inversions are based on the recurring interactions of the *b* locus with 43-45 chromosomal segment (3/18 or 16.7 %) and on its scarce interactions with 22 or 56 chromosomal sections, respectively. These data show that the “sensitive microvolume” suggested can include one or another of these sections in one or the other of sperm nucleus and the type of the alternative “partner” with which the *b* locus interacts is obviously determined by chance.

2D model of *Drosophila* autosome 2 based on the *b* inversions.

Using data on the *b* inversions and basic approaches to 2D modeling elaborated for the *vg* inversions (Alexandrov *et al.*, 2007b) the large-scale geometry of elementary fiber of the chromosome 2 in *Drosophila* sperm genome was constructed. Thereat, the chromosome “hot” nodes with which the *b* gene repeatedly (40-41, 35-36 and 43-45 regions) or singly

(22 and 56 sections) interacts were stood out and the average distances r_i of interaction of each “hot” node with the *b* gene were calculated with regard to the number of interaction observed (Table 1) using the equation proposed earlier (Alexandrov *et al.*, 2007b).

As the end result of modeling shows, the proximity of the *b* gene region (2) with centromeric heterochromatin (1), 35-36 (3), 43-45 (4), 22 (5) and 56 (6) regions (Figure 1A) results in model the main features of which are entirely consistent with the megarosette-loop configuration proposed earlier for this autosome on the basis of data for the *vg* inversions. Moreover, the possibility of contact and induced interaction of the *b* locus with both peritelomeric sections (22 and 56) should expect on the basis of this configuration where the both telomeric ends of chromosome were close to centromeric heterochromatin too (Alexandrov *et al.*, 2007b).

General 2D model of autosome 2 based on the both *b* and *vg* inversions.

The same megarosette-loop configuration of autosome 2 revealed independently by the both set of inversion data permits to create a general 2D model of autosome 2 in *Drosophila* sperm genome by means of superposition of two special 2D models based on the *b* (see above) and *vg* inversions (Alexandrov *et al.*, 2007b). The results of such superposition are presented in Figure 1B.

As it is seen, the generalized model guided by the “hot” chromosome nodes with which the *b* and *vg* regions most frequently interact after irradiation shows with the utmost clarity the first principles of spatial organization of haploid autosome 2 in *Drosophila* sperm genome in the form of a megarosette-loop structure as an united whole.

It is important to note that in this structure the middles of 2L and 2R arms of autosome 2 were most frequently close to their own centromeric heterochromatin in sperm nuclei at the time of irradiation giving rise, arbitrarily speaking, to the “sensitive microvolume” within of which the *b* region can occasionally interact with 2R arm centromeric heterochromatin and the *vg* one can do the same with 2L arm heterochromatin.

Simultaneously, these data testify that this “sensitive microvolume” must necessary include 2L and 2R arm telomeric ends too. Therefore, centromeric heterochromatin and at least four euchromatic areas

(the *b* and *vg* genes with neighbouring regions as well as the 2L and 2R arm telomeric regions) which are far apart on the molecular (DNA) map of autosome 2 but spatially close to each other within sperm genome might interact each other with the certain probability determined evidently by their 3D-position and the distance between interacted pairs in the given sperm nucleus.

The employment of all euchromatic sites with which the *vg* region interacts after irradiation (Alexandrov *et al.*, 2007b, Table 1) i.e. including these sites into the *vg*

“sensitive microvolume” during modeling gives rise to more compact generalized 2D model in which formerly relaxed euchromatic areas turn out quite near with each other (not shown). This may create the prerequisites for interaction of such regions if they contain radiation-induced lesions with formation of the appropriate inversions not associated with the locus-specific ones. The detection of the formers may be not only confirm the spatial proximity of these euchromatic areas but also get a new independent evidences for megarosette-loop model proposed as a whole.

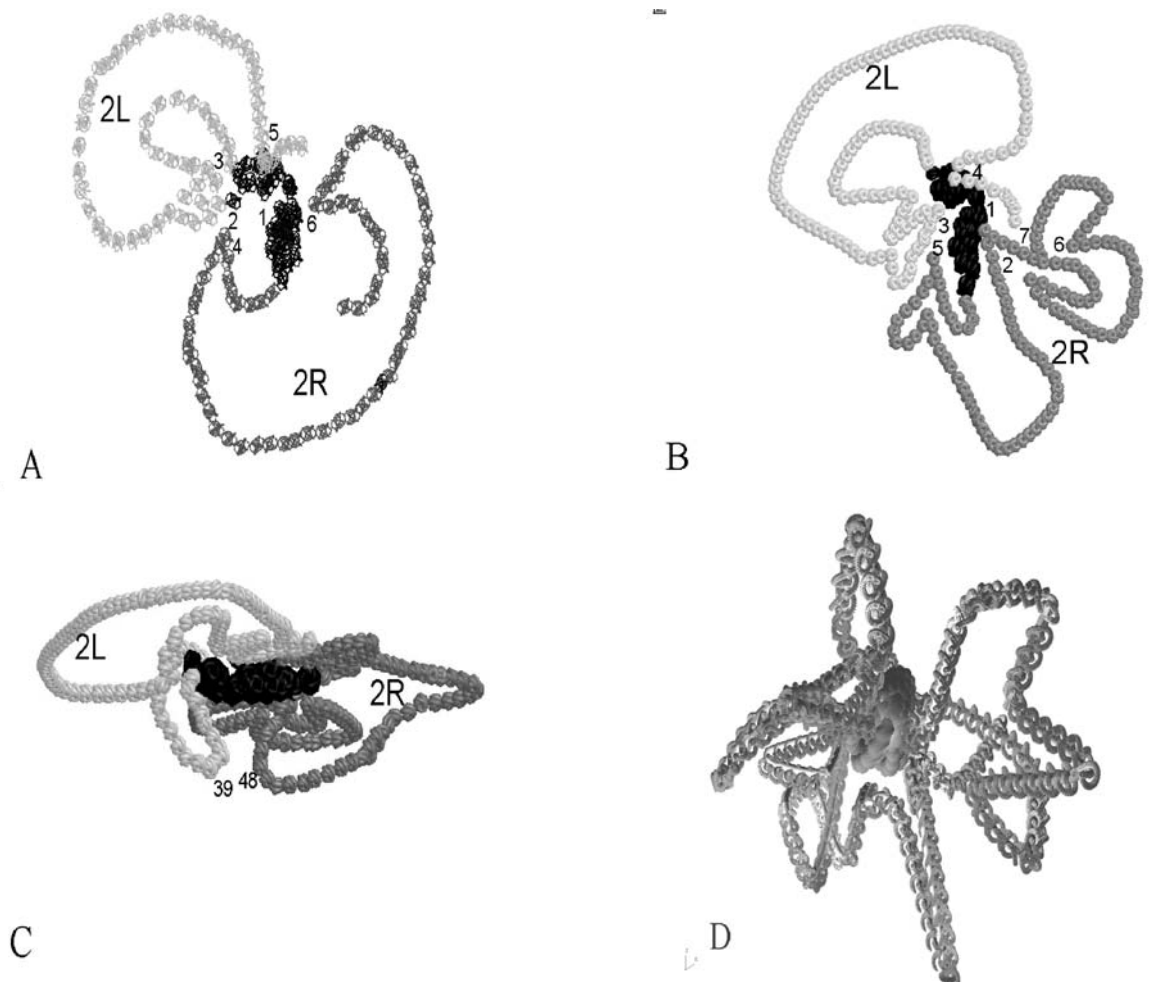


Figure 1. (A) 2D model of autosome 2 in *Drosophila* sperm genome based on the induction pattern of the *b* inversions induced by γ -rays of ^{60}Co or 0.85 MeV fission neutrons (details see text). (B) A general 2D model of autosome 2 based on both *b* and *vg* inversion data: 1 - centromeric heterochromatin; 2, 3, 4, 5, 6 and 7 - the *vg*, *b*, 22, 43-44, 56 and 60 regions, respectively. (C) A general 2D model rotated by 25° about the horizontal X axis on oneself to show 39 and 48 regions approached each other. (D) Example of a general 3D model of an elementary fiber of autosome 2 in *Drosophila* sperm genome constructed on the basis of approaches described earlier (Alexandrov *et al.*, 2007b). As an idealization, throughout these models all loops without inversion breakpoints are relaxed.

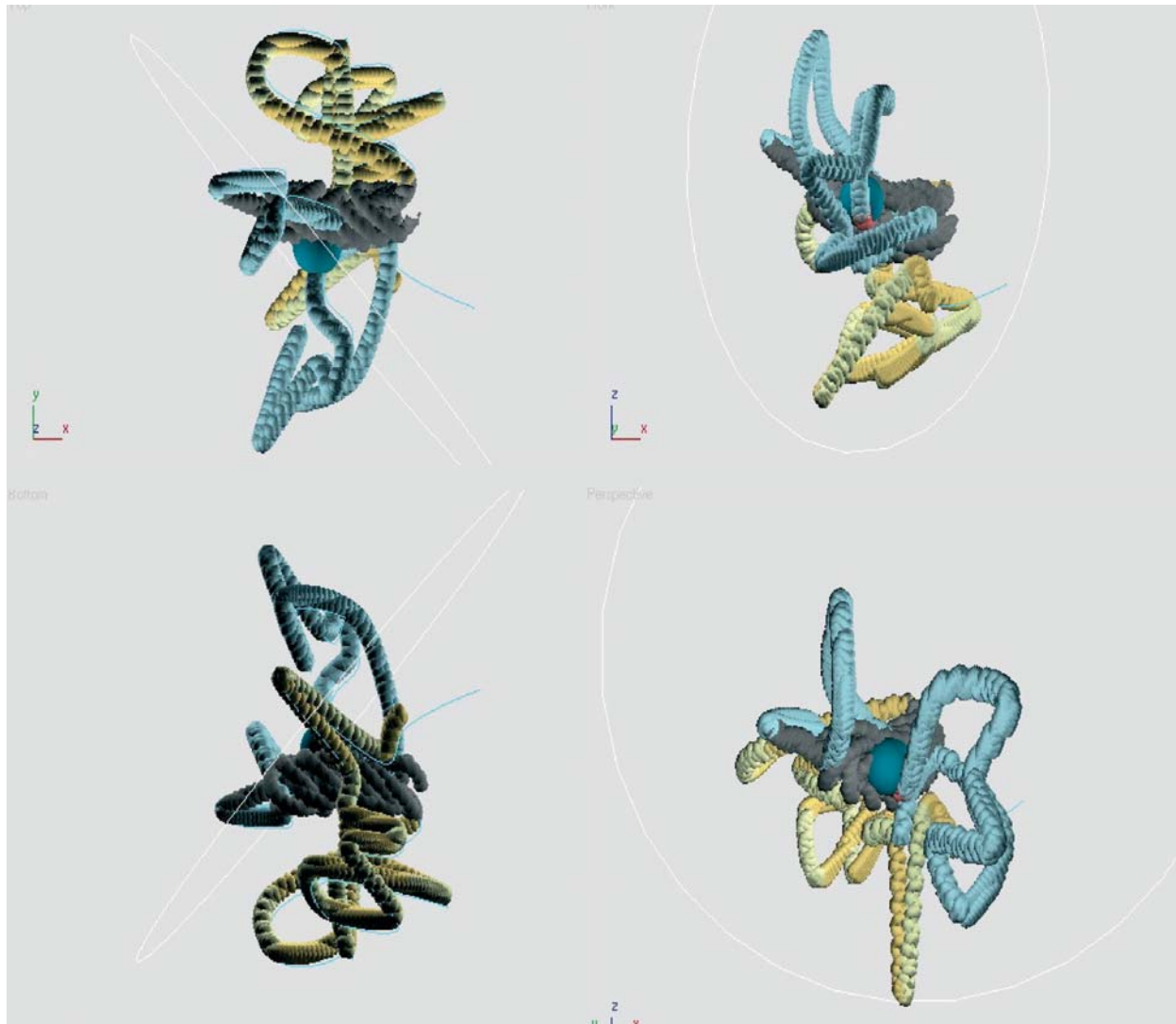


Figure 2. A colored 3D model of megarosette-loop structure for autosome 2 in *Drosophila* sperm genome displayed in the top (overhead at the left), front (overhead at the right), bottom (at the lower left) and perspective (at the lower right) planes.

Non-locus-specific inversions.

The expectations above mentioned were entirely realized if one will now look at the induction patterns of 19 inversions occasionally occurring in genome of the “point” *b*, *cn* or *vg* mutants induced by different quality radiation and scored at the same experiments (Table 2).

As these data show, the independent occurrence of inversions with the breakpoints at the middle region of 2L arm (section 35 adjacent to the *b* gene) and centromeric heterochromatin (section 40-41) within the

genome of the *b* (one case) and *vg* (two cases) “point” mutants is reasonably expectative with the proximity of the *b* gene and centromeric heterochromatin resulting from the induction pattern of the *b* inversions described above. A repetitive occurrence of the paracentric inversions based on the interaction of peritelomeric region (section 22-23 of 2L arm) with a middle of the same arm (section 34-36) within genome of the *cn* (four cases) and *vg* (one case) “point” mutants is well regular trend guided by the proximity of the four euchromatic areas above mentioned. Also, five cases of interaction of the 2R arm centromeric heterochromatin (section 41) with the euchromatic sections 50, 52, 58 and 60

resulting in the attendant inversions within the genome of the “point” mutants in question are entirely consistent with the spatial configuration of the 2R arm of autosome 2 predetermined by the induction pattern of the *vg* inversions (Alexandrov et al., 2007a, b). The emergence of rest five inversions within genome of the *b*, *cn* and *vg* “point” mutants is in line with the global autosome 2 configuration suggested and reflects a possibility of formation a small loops within a “giant” ones. The detection of pericentric inversion based on the interaction of 39 section (pericentromeric region of 2L arm) with 48 one (neighbouring with *vg* region in 2R arm) within genome of the *vg* “point” mutant (Table 2) implies proximity of these 2L and 2R regions in this sperm nucleus at the time of irradiation. The spatial point where two regions in question come within short distances of each other obvious to lie rather in other plane than that for a general 2D model depicted, for example, in the background of the model. Visualization of such points is quite possible if a general model will be rotated by 25° about the horizontal X axis on oneself (Figure 1C). A visual (black-white) 3D model in the perspective plane constructed on the basis of approaches described earlier (Alexandrov et al., 2007b) is shown in Figure 1D and its colored versions in different planes are depicted in Figure 2.

Conclusion

All our unique data on the patterns of radiation-induced locus-specific inversions in *Drosophila* autosome 2 as a part of sperm genome discussed above and earlier (Alexandrov et al., 2007a, b) unequivocally indicate that the certain chromosomal regions radiation damage of which brings about para- and pericentric inversions have located non-random relatively each other within the sperm nucleus showing ordered organization of entire chromosome. The peculiarities of distribution of the second inversion breakpoints relative to the fixed first break have permitted to us to create the model of spatial arrangement of the chromosome studied in sperm nucleus in the form of the megarosette-loop structure.

The major and specific feature of structure proposed is alignment of telomeric ends as well as a middle of arms of this metacentric autosome around the centromeric heterochromatin resulting in the most compact formation. Incidentally there are all reasons to believe that all other chromosomes in sperm genome have the same spatial organization which is unlike Rabl's configuration of interphase chromosomes in

animal somatic as well as *Drosophila* embryonic cells (Ellison and Howard, 1981).

It may anticipate that Rabl's configuration is as yet persisted in early spermatids after completion of the meiotic divisions at least in *Drosophila* early spermiogenesis. In such case, the conversion of this chromosome configuration to megarosette-loop structure must keep pace with chromatin remodeling in late spermiogenesis where the processes of histone-protamine transition are recently identified in details (Kimmins and Sassone-Corsi, 2005). Now, our pioneering studies described enable to believe that the protein remodeling of chromatin in male germ cells is accompanied with its global and deep spatial reorganization details of which (molecular mechanisms and forces guiding this reorganization, the meaning of DNA sequences etc.), however, remain an enigma so far.

References

- Adams MD, Celniker SE, Holt RA et al. The genome sequence of *Drosophila melanogaster*. *Science*. 287: 2185-2195, 2000.
- Alexandrov ID, Alexandrova MV. The genetic and cytogenetic boundaries of the radiation-induced rearrangements scored as lethal *black* mutations in *D. melanogaster*. *Drosophila Inform. Service*. 70: 16-19, 1991.
- Alexandrov ID, Alexandrova MV, Korablinova SV, Korovina LN. Spatial arrangement of the animal male germ cell genome: I. Non-random pattern of radiation-induced inversions involving the *vestigial* region in autosome 2 of *Drosophila melanogaster*. *Advances in Molecular Biology*. 1: 23-29, 2007a.
- Alexandrov ID, Stepanenko VA, Alexandrova MV. 39 spatial arrangement of the animal male germ cell genome: II. 2D-3D simulation and visualization of spatial configuration of major chromosome 2 in *Drosophila* sperm. *Advances in Molecular Biology*. 1: 71-77, 2007b.
- Alexandrov ID, Zakharov IA, Alexandrova MV. The Moscow Regional *Drosophila melanogaster* Stock Center. *Drosophila Inform. Service*. 80: 109-130, 1997.
- Ellison JR and Howard GC. Non-random position of the A-T rich DNA sequences in the early embryos of *Drosophila virilis*. *Chromosoma*. 83: 555-561, 1981

Kimmins S, Sassone-Corsi P. Chromatin remodeling and epigenetic features of germ cells. *Nature*. 434: 583-589, 2005.

Lefevre G Jr. A photographic representstion and interpretation of the polytene chromosomes of *Drosophila melanogaster* salivary glands. In: The Genetic and Biology of *Drosophila*. M. Ashburner and E. Novitski (Eds.). Acad. Press. London, V. 1a: 31-66, 1976.

Rabl C. Über Zelltheilung. *Morphologisches Jahrbuch*. 10: 214-330, 1885.